

Hamed Bagheri¹, Yaser Kiani ², Mohammad Reza Eslami¹

Buckling of moderately thick annular plates subjected to torque

An attempt is made in the current research to obtain the fundamental buckling torque and the associated buckled shape of an annular plate. The plate is subjected to a torque on its outer edge. An isotropic homogeneous plate is considered. The governing equations of the plate in polar coordinates are established with the aid of the Mindlin plate theory. Deformations and stresses of the plate prior to buckling are determined using the axisymmetric flatness conditions. Small perturbations are then applied to construct the linearised stability equations which govern the onset of buckling. To solve the highly coupled equations in terms of displacements and rotations, periodic auxiliary functions and the generalised differential quadrature method are applied. The coupled linear algebraic equations are a set of homogeneous equations dealing with the buckling state of the plate subjected to a unique torque. Benchmark results are given in tabular presentations for combinations of free, simply-supported, and clamped types of boundary conditions. It is shown that the critical buckling torque and its associated shape highly depend upon the combination of boundary conditions, radius ratio, and the thickness ratio.

1. Introduction

Circular and annular plates under the action of a torque appear frequently as parts of transmissions, pump rotors, and compressors. Dean [1] investigated the elastic buckling of annular plates under uniform shearing force applied on its edges. The mentioned work is the fundamental investigation on the stability of annular plates under shear stresses. The theoretical investigation of this work is limited to thin plates with both inner and outer edges clamped. Using the Galerkin

✉ Yaser Kiani, e-mail: y.kiani@sku.ac.ir

¹Mechanical Engineering Department, Amirkabir University of Technology, Tehran, Iran.

²Faculty of Engineering, Shahrekord University, Shahrekord, Iran.



method and the Hsu criterion, Tani et al. [2] investigated the parametric instability of annular plates under periodic torsion. The instability regions associated with both principal and combination parametric resonances are clarified for relatively low frequency ranges. It is found that under the purely periodic torsion only the combination instability region exists, while under the simultaneous action of the static torsion the principal instability region exists too. The circumferential phase difference of two vibration modes excited simultaneously at the resonance is also found to change remarkably the relative width of the instability region. Tani [3] also theoretically analyzed the dynamic stability of clamped, polar orthotropic annular plates under the action of pulsating torsion where the effect of the static torsion was taken into consideration by the Galerkin method. Durban and Stavsky [4] presented an analytical closed-form solution for the critical buckling shear stress of thin polar orthotropic annular plates using the classical plate theory formulation. Detailed results for the critical load are provided for a wide range of material parameters, plate geometry, and various boundary conditions.

For plates with variable thickness, Irie et al. [5] obtained the frequencies and buckling loads of annular plate subjected to a torque. Numerical results of this study are obtained according to the Ritz method. For this purpose, the transverse deflection of an annular plate is written in a series of the deflection functions of a uniform thickness annular plate without the action of a torque. The kinetic and strain energies of the plate are evaluated analytically and the frequency equation of the plate is derived using the stationary value of the Lagrange functional. The present method is applied to annular plates with two types of radial thickness variation, i.e., power law and exponential, and the natural frequencies (the frequency parameters) and the divergence torques are calculated numerically. As a result, the effects of the varying thickness, inner to outer radii ratio, and the boundary conditions may be explored. In another study, Irie et al. [6] reported the buckling loads of uniform thickness annular plates subjected to a torque. The buckling torques and the buckling wave numbers in the circumferential direction are reported for different radius ratios and for all combinations of clamped, simply supported, and free boundary conditions. These values have been obtained by the Ritz method. The numerical results of this study, however, are limited to the case of thin plates where the effects of transverse shear stresses are ignored. The obtained numerical results, therefore, may not be accurate for moderately thick and thick plates.

Zajączkowski [7] presented an investigation on the parametric instability of elastic annular plates subjected to periodic torques on both inner and outer edges. Instability charts are provided in graphical presentations. Doki and Tani [8] analysed the interactive buckling of annular plates made from a polar orthotropic material under the combined action of radial and shear stresses. This study is limited to the case of annular plates with both edges clamped. The deflected shape of the plate is written as a series of shape functions, where each one satisfies the clamping conditions. The Galerkin method is applied to the governing stability equation of the plate to reach a standard eigenvalue problem. Hamada and Harima [9]

applied the conventional finite difference method to the governing equations of a shear deformable plate to extract the shear buckling stresses of annular plates with arbitrary combination of edge supports. Various combinations of clamped, simply-supported, and free edges are examined. In this research, also an experimental investigation is performed for plates with both edges clamped. Ore and Durban [10] analysed the buckling of a torque-loaded annular plate considering the elasto-plastic material behaviour for the plate. This study covers both clamped and simply supported edges. The governing equations consist of the classical stability equation of thin plates in conjunction with the small strain J_2 flow rule of plasticity or the deformation theory of plasticity. This study also presents an experimental procedure to obtain the critical shear loads.

Chang-jun and Xiao-an [11, 12] studied the buckling and post-buckling of annular plates subjected to in-plane shear. The post-buckling analysis is based on the Liapunov-Schmidt procedure and perturbation expansions in a small parameter to seek the bifurcation solutions of the non-linear boundary value problem and to study the post-buckling behaviour of an annular plate under shear forces. Singhatanadgid and Ungbhakorn [13] derived the similitude invariants and scaling laws for buckling of polar orthotropic annular plates subjected to torsional loads and/or radial compression. Buckling behaviours of the prototype with complicated boundary conditions, of which a theoretical solution is not available, can be predicted from the experimental result on the model. Torsional vibration behaviour is studied by Wu [14]. An analytical model is developed, and the natural frequencies and mode shapes are calculated for the torsional vibration under different boundary conditions. An exact procedure is developed to obtain the torsional frequencies of the plate in terms of the Bessel functions. Maretic et al. [15] investigated the transverse vibration of a thin annular plate which is clamped at its inner edge to a rigid shaft, while its outer edge is clamped to a rigid cylinder. The shaft and the outer edge of the plate are loaded by torques of the same intensity, but of opposite directions. The whole structure rotates at a constant angular speed. The majority of the work is devoted to the influence of the applied torque on the natural frequencies. Simultaneous interaction of the forces due to rotation and shear stresses caused by torque are investigated.

The above literature survey and further investigation of the available works through the open literature reveals that a comprehensive study on the asymmetrical buckling of shear deformable annular plates under the action of shear stresses is not reported so far. To this end, an annular plate which is subjected to a torque on its outer edge is considered. Mindlin plate theory is used to estimate the components of displacement field. The equations associated with the primary state and buckling state are obtained. The critical state of the plate are obtained by means of the generalised differential quadrature method. The provided solution method may be used for arbitrary combinations of free, clamped, and simply supported boundary conditions. Tabulated numerical results provide the critical buckling torque as function of the thickness ratio, radius ratio, and boundary conditions.

2. Theoretical formulation

An isotropic homogeneous annular plate is under investigation. Inner radius, outer radius, and thickness of the plate are denoted by b , a , and h . Polar coordinates system (r, θ, z) is applied to the plate where the origin is located at the midsurface center of the plate. In the present research, the radial, circumferential and through-the-thickness directions of the plate are denoted by r , θ , and z represent, respectively.

Mindlin plate theory is used in the current research to obtain the components of the displacement field in the annular plate. This theory is accurate enough in prediction of the global characteristics of beams, plates, and shells. Using the Mindlin plate theory, the three components of the displacement field may be expressed in terms of displacement of the mid-surface and also cross-section rotations as [16–18]

$$\begin{aligned} u(r, \theta, z) &= u_0(r, \theta) + z\phi_r(r, \theta), \\ v(r, \theta, z) &= v_0(r, \theta) + z\phi_\theta(r, \theta), \\ w(r, \theta, z) &= w_0(r, \theta), \end{aligned} \quad (1)$$

where as usual, in Eqs. (1) u , v , and w represent the radial, circumferential, and through-the-thickness displacement components, respectively. A subscript 0 indicates the characteristics of the mid-surface. As usual, ϕ_r and ϕ_θ stand for the transverse normal rotations about θ and r axes, respectively. In all of the manuscript, same as Eq. (1) a letter after comma means the partial derivative with respect to that letter.

The strain field of an annular plate suitable for first order shear deformation plate theory are expressed as [16, 17]

$$\begin{aligned} \varepsilon_{rr} &= u_{,r} + \frac{1}{2}w_{,r}^2, \\ \varepsilon_{\theta\theta} &= \frac{1}{r}u + \frac{1}{r}v_{,\theta} + \frac{1}{2r^2}w_{,\theta}^2, \\ \gamma_{r\theta} &= \frac{1}{r}u_{,\theta} + v_{,r} - \frac{1}{r}v + \frac{1}{r}w_{,\theta}w_{,r}, \\ \gamma_{rz} &= u_{,z} + w_{,r}, \\ \gamma_{z\theta} &= \frac{1}{r}w_{,\theta} + v_{,z}. \end{aligned} \quad (2)$$

In Eq. (2), radial and circumferential strains are denoted by ε_{rr} and $\varepsilon_{\theta\theta}$. Besides, the components of the shear strain are shown by $\gamma_{r\theta}$, γ_{rz} , and $\gamma_{z\theta}$.

The constitutive equation of the plate under linear elastic deformation are as [16]

$$\begin{Bmatrix} \sigma_{rr} \\ \sigma_{\theta\theta} \\ \tau_{r\theta} \\ \tau_{rz} \\ \tau_{z\theta} \end{Bmatrix} = \begin{bmatrix} Q_{11} & Q_{12} & 0 & 0 & 0 \\ Q_{12} & Q_{22} & 0 & 0 & 0 \\ 0 & 0 & Q_{44} & 0 & 0 \\ 0 & 0 & 0 & Q_{55} & 0 \\ 0 & 0 & 0 & 0 & Q_{66} \end{bmatrix} \begin{Bmatrix} \varepsilon_{rr} \\ \varepsilon_{\theta\theta} \\ \gamma_{r\theta} \\ \gamma_{rz} \\ \gamma_{z\theta} \end{Bmatrix}, \quad (3)$$

where in the above equation Q_{ij} , $i, j = 1, 2, 4, 5, 6$ are the material stiffness coefficients. For an isotropic homogeneous material, these coefficients may be obtained in terms of the Young modulus E and Poisson's ratio ν as

$$\begin{aligned} Q_{11} = Q_{22} &= \frac{E}{1 - \nu^2}, & Q_{12} &= \nu Q_{11}, \\ Q_{44} = Q_{55} = Q_{66} &= \frac{E}{2(1 + \nu)}. \end{aligned} \quad (4)$$

2.1. Stress resultants

Stress resultants of the plate may be revealed upon integration of the stress field through the thickness of the plate [19]. Therefore, the stress resultants of the plate under first order shear deformation plate theory take the form

$$\begin{aligned} (N_{rr}, N_{\theta\theta}, N_{r\theta}) &= \int_{-h/2}^{+h/2} (\sigma_{rr}, \sigma_{\theta\theta}, \tau_{r\theta}) \, dz, \\ (M_{rr}, M_{\theta\theta}, M_{r\theta}) &= \int_{-h/2}^{+h/2} z(\sigma_{rr}, \sigma_{\theta\theta}, \tau_{r\theta}) \, dz, \\ (Q_r, Q_\theta) &= \int_{-h/2}^{+h/2} (\tau_{rz}, \tau_{z\theta}) \, dz. \end{aligned} \quad (5)$$

Definition of stress resultants in terms of mid-surface degrees of freedom may be achieved by substitution of Eq. (3) into Eqs. (5) with the aid of Eqs. (1) and (2).

Therefore one has

$$\begin{aligned}
 \begin{Bmatrix} N_{rr} \\ N_{\theta\theta} \\ N_{r\theta} \end{Bmatrix} &= \begin{bmatrix} A_{11} & A_{12} & 0 \\ A_{12} & A_{22} & 0 \\ 0 & 0 & A_{66} \end{bmatrix} \begin{Bmatrix} u_{0,r} + \frac{1}{2}w_{0,r}^2 \\ \frac{1}{r}v_{0,\theta} + \frac{1}{r}u_0 + \frac{1}{2r^2}w_{0,\theta}^2 \\ \frac{1}{r}u_{0,\theta} + v_{0,r} - \frac{1}{r}v_0 + \frac{1}{r}w_{0,r}w_{0,\theta} \end{Bmatrix}, \\
 \begin{Bmatrix} M_{rr} \\ M_{\theta\theta} \\ M_{r\theta} \end{Bmatrix} &= \begin{bmatrix} D_{11} & D_{12} & 0 \\ D_{12} & D_{22} & 0 \\ 0 & 0 & D_{66} \end{bmatrix} \begin{Bmatrix} \phi_{r,r} \\ \frac{1}{r}\phi_r + \frac{1}{r}\phi_{\theta,\theta} \\ \frac{1}{r}\phi_{r,\theta} + \phi_{\theta,r} - \frac{1}{r}\phi_\theta \end{Bmatrix}, \\
 \begin{Bmatrix} Q_r \\ Q_\theta \end{Bmatrix} &= \begin{bmatrix} A_{55} & 0 \\ 0 & A_{44} \end{bmatrix} \begin{Bmatrix} w_{0,r} + \phi_r \\ \frac{1}{r}w_{0,\theta} + \phi_\theta \end{Bmatrix}.
 \end{aligned} \tag{6}$$

For an isotropic homogeneous material, the extensional stiffnesses A_{ij} and the bending stiffnesses D_{ij} may be written in terms of the Young's modulus, plate thickness and Poisson's ratio. These constants are as follows

$$\begin{aligned}
 A_{11} = A_{22} &= \frac{Eh}{1-\nu^2}, \quad A_{12} = \frac{\nu Eh}{1-\nu^2}, \quad A_{44} = A_{55} = A_{66} = \frac{Eh}{2(1+\nu)}, \\
 D_{11} = D_{22} &= \frac{Eh^3}{12(1-\nu^2)}, \quad D_{12} = \frac{\nu Eh^3}{12(1-\nu^2)}, \quad D_{66} = \frac{Eh^3}{24(1+\nu)}.
 \end{aligned} \tag{7}$$

2.2. Equilibrium equations and boundary conditions

Static version of the Hamilton principle, also known as the virtual displacement principle, may be used to obtain the nonlinear equilibrium equations of the plate [19]. The total virtual energy of the plate consists of two parts. The first part, which is the virtual strain energy, and the second one, which is the potential energy due to the applied torque on the outer edge of the annular plate. Consequently for an equilibrium position, the following identity should be satisfied

$$\begin{aligned}
 \int_b^a \int_0^{2\pi} \int_{-h/2}^{+h/2} (\sigma_{rr}\delta\varepsilon_{rr} + \sigma_{\theta\theta}\delta\varepsilon_{\theta\theta} + \tau_{r\theta}\delta\gamma_{r\theta} + \tau_{z\theta}\delta\gamma_{z\theta} + \tau_{rz}\delta\gamma_{rz}) r \, dz \, d\theta \, dr \\
 - \frac{T}{2\pi a^2} \int_0^{2\pi} r \delta v_0|_{r=a} \, d\theta = 0.
 \end{aligned} \tag{8}$$

With the aid of proper mathematical manipulations and simplifications, the governing equilibrium equations of the plate are obtained as follows

$$\begin{aligned}
 \delta u_0 : N_{rr,r} + \frac{1}{r}N_{r\theta,\theta} + \frac{1}{r}(N_{rr} - N_{\theta\theta}) &= 0, \\
 \delta v_0 : \frac{1}{r}N_{\theta\theta,\theta} + N_{r\theta,r} + \frac{2}{r}N_{r\theta} &= 0, \\
 \delta w_0 : Q_{r,r} + \frac{1}{r}Q_{\theta,\theta} + \frac{1}{r}Q_r + N_{rr}w_{0,rr} + N_{\theta\theta} \left(\frac{1}{r}w_{0,r} + \frac{1}{r^2}w_{0,\theta\theta} \right) \\
 + 2N_{r\theta} \left(\frac{1}{r}w_{0,r\theta} - \frac{1}{r^2}w_{0,\theta} \right) &= 0, \\
 \delta \phi_r : M_{rr,r} + \frac{1}{r}M_{r\theta,\theta} + \frac{1}{r}(M_{rr} - M_{\theta\theta}) - Q_r &= 0, \\
 \delta \phi_\theta : \frac{1}{r}M_{\theta\theta,\theta} + M_{r\theta,r} + \frac{2}{r}M_{r\theta} - Q_\theta &= 0.
 \end{aligned} \tag{9}$$

The boundary conditions of the plate may be obtained through the process of applying the Green-Gauss theorem to the total virtual energy of the plate. The boundary conditions are two sets. The in-plane and out-of-plane boundary conditions. The in-plane boundary conditions of the plate for the current problem are as follows

$$\begin{aligned}
 r = b : u_0 = v_0 &= 0, \\
 r = a : u_0 = N_{r\theta} - \frac{T}{2\pi a^2} &= 0.
 \end{aligned} \tag{10}$$

The above boundary conditions indicate a plate which is subjected to a conservative torque on the outer edge while the inner edge is restrained against radial and circumferential displacements.

The out-of-plane boundary conditions are used for the onset of buckling. Three different types of boundary conditions are used in this study, which are clamped (C), simply supported (S), and free (F). The out-of plane boundary conditions for each type may be expressed as

$$\begin{aligned}
 S : w_0 = M_{rr} = \phi_\theta &= 0, \\
 C : w_0 = \phi_r = \phi_\theta &= 0, \\
 F : rQ_r + rN_{rr}w_{0,r} + N_{r\theta}w_{0,\theta} = M_{rr} = M_{r\theta} &= 0.
 \end{aligned} \tag{11}$$

3. Prebuckling analysis

An accurate and correct prebuckling analysis is a vital step to obtain the buckling load and shape of the plate. Prebuckling analysis should be done to designate the stresses and deformations of the plate before and also at the onset

of buckling. Only flat pre-buckling configurations are taken into account, where the classical bifurcation buckling may be extracted under such circumstances. Consequently, in prebuckling state, $w_0^0 = \phi_r^0 = \phi_\theta^0 = 0$ where a superscript 0 indicates the prebuckling state of the plate. It is of worth-noting that, to obtain the prebuckling state of the plate, solution of the first two equations is sufficient.

Due to the presence of a constant torque, symmetrical geometry, and boundary conditions the prebuckling deformations are also symmetric. The prebuckling stresses of the plate should be obtained according to the first two of the equilibrium equations under symmetrical deformations. These equations in prebuckling state are

$$\begin{aligned} N_{rr,r}^0 + \frac{1}{r}(N_{rr}^0 - N_{\theta\theta}^0) &= 0, \\ N_{r\theta,r}^0 + \frac{2}{r}N_{r\theta}^0 &= 0, \end{aligned} \quad (12)$$

The second equation is a simple ordinary differential equation in terms of $N_{r\theta}^0$. Recalling the boundary conditions $2\pi a^2 N_{r\theta}^0(a) = T$, the solution of this equation may be expressed as $2\pi r^2 N_{r\theta}^0(a) = T$. This equation also may be written in terms of tangential displacement v_0^0 which is a second order equation whose solution, recalling the boundary conditions (10), takes the form

$$v_0^0 = \frac{T(1 + \nu)}{2\pi b^2 r E h} (r^2 - b^2). \quad (13)$$

Similarly, the first of Eqs. (12) results in a simple homogeneous differential equation for u_0^0 as

$$\frac{du_0^{02}}{dr^2} + \frac{1}{r} \frac{du_0^0}{dr} - \frac{1}{r^2} u_0^0 = 0. \quad (14)$$

Recalling the boundary conditions $u_0^0(a) = u_0^0(b) = 0$, the solution of the above equation may be written as

$$u_0^0 = 0. \quad (15)$$

Using Eqs. (13) and (15), the stress resultants of the prebuckling state may be obtained as

$$\begin{aligned} N_{rr}^0 &= 0, \\ N_{\theta\theta}^0 &= 0, \\ N_{r\theta}^0 &= \frac{T}{2\pi r^2}, \end{aligned} \quad (16)$$

The above equation accepts the fact that, prior to buckling and due to an applied torque, only an in-plane shear stress is induced and the components of radial and circumferential stresses are equal to zero.

4. Stability equations

Stability equations govern the onset of buckling of the plate. These equations may be obtained using the small perturbations or the adjacent equilibrium criterion [22, 23]. A plate whose displacement field in prebuckling state are u_0^0 , v_0^0 , w_0^0 , ϕ_r^0 , and ϕ_θ^0 is considered. Small perturbations are applied to the components of the prebuckling state which are denoted by u_0^1 , v_0^1 , w_0^1 , ϕ_r^1 , and ϕ_θ^1 . Consequently, components of displacement on the secondary equilibrium path are

$$\begin{aligned}
 u_0 &= u_0^0 + u_0^1, \\
 v_0 &= v_0^0 + v_0^1, \\
 w_0 &= w_0^0 + w_0^1, \\
 \phi_r &= \phi_r^0 + \phi_r^1, \\
 \phi_\theta &= \phi_\theta^0 + \phi_\theta^1.
 \end{aligned} \tag{17}$$

The incremental displacement which are shown by a superscript 1 are sufficiently small since only the buckling state in under investigation. Similar to displacements, the incremental stress resultants are also obtained [22, 23]. The governing stability equations which govern the onset of buckling take the form

$$\begin{aligned}
 N_{rr,r}^1 + \frac{1}{r} N_{r\theta,\theta}^1 + \frac{1}{r} (N_{rr}^1 - N_{\theta\theta}^1) &= 0, \\
 N_{r\theta,r}^1 + \frac{1}{r} N_{\theta\theta,\theta}^1 + \frac{2}{r} N_{r\theta}^1 &= 0, \\
 Q_{r,r}^1 + \frac{1}{r} Q_{\theta,\theta}^1 + \frac{1}{r} Q_r^1 + N_{rr}^0 w_{0,rr}^1 + N_{\theta\theta}^0 \left(\frac{1}{r} w_{0,r}^1 + \frac{1}{r^2} w_{0,\theta\theta}^1 \right) \\
 + 2N_{r\theta}^0 \left(\frac{1}{r} w_{0,r\theta}^1 - \frac{1}{r^2} w_{0,\theta}^1 \right) &= 0, \\
 M_{rr,r}^1 + \frac{1}{r} M_{r\theta,\theta}^1 + \frac{1}{r} (M_{rr}^1 - M_{\theta\theta}^1) - Q_r^1 &= 0, \\
 M_{r\theta,r}^1 + \frac{1}{r} M_{\theta\theta,\theta}^1 + \frac{2}{r} M_{r\theta}^1 - Q_\theta^1 &= 0.
 \end{aligned} \tag{18}$$

The expression of the stability equations in terms of the displacements may be obtained easily as

$$\begin{aligned}
 & A_{11} \left(u_{0,rr}^1 + \frac{1}{r} u_{0,r}^1 + \frac{1}{r} v_{0,r\theta}^1 - \frac{1}{r^2} u_0^1 - \frac{1}{r^2} v_{0,\theta}^1 \right) \\
 & \quad + A_{66} \left(\frac{1}{r^2} u_{0,\theta\theta}^1 - \frac{1}{r} v_{0,r\theta}^1 - \frac{1}{r^2} v_{0,\theta}^1 \right) = 0, \\
 & A_{11} \left(\frac{1}{r} u_{0,r\theta}^1 + \frac{1}{r^2} u_{0,\theta}^1 + \frac{1}{r^2} v_{0,\theta\theta}^1 \right) \\
 & \quad + A_{66} \left(-\frac{1}{r^2} u_{0,r\theta}^1 - \frac{1}{r} u_{0,r\theta}^1 + \frac{1}{r} v_{0,r}^1 - \frac{1}{r^2} v_0^1 + v_{0,rr}^1 \right) = 0, \\
 & A_{66} \left(\phi_{r,r}^1 + \frac{1}{r} \phi_{\theta,\theta}^1 + \frac{1}{r} \phi_r^1 + \frac{1}{r^2} w_{0,\theta\theta}^1 + w_{0,rr}^1 + \frac{1}{r} w_{r,r}^1 \right) \\
 & \quad + \frac{T}{\pi r^2} \left(\frac{1}{r} w_{0,r\theta}^1 - \frac{1}{r^2} w_{0,\theta}^1 \right) = 0, \tag{19} \\
 & D_{11} \left(\phi_{r,rr}^1 + \frac{1}{r} \phi_{r,r}^1 + \frac{1}{r} \phi_{\theta,r\theta}^1 - \frac{1}{r^2} \phi_r^1 - \frac{1}{r^2} \phi_{\theta,\theta}^1 \right) \\
 & \quad + D_{66} \left(\frac{1}{r^2} \phi_{r,\theta\theta}^1 - \frac{1}{r} \phi_{\theta,r\theta}^1 - \frac{1}{r^2} \phi_{\theta,\theta}^1 \right) - A_{66} \left(\phi_r^1 + w_{0,r}^1 \right) = 0, \\
 & D_{11} \left(\frac{1}{r} \phi_{r,r\theta}^1 + \frac{1}{r^2} \phi_{r,\theta}^1 + \frac{1}{r^2} \phi_{\theta,\theta\theta}^1 \right) + D_{66} \left(\frac{1}{r^2} \phi_{r,\theta}^1 - \frac{1}{r} \phi_{r,r\theta}^1 + \frac{1}{r} \phi_{\theta,r}^1 \right. \\
 & \quad \left. - \frac{1}{r^2} \phi_{\theta}^1 + \phi_{\theta,rr}^1 \right) - A_{66} \left(\phi_{\theta}^1 + \frac{1}{r} w_{0,\theta}^1 \right) = 0.
 \end{aligned}$$

Eqs. (19) are a set of linearised equations in terms of the displacement components. These equations act as a set of homogeneous equations in terms of the incremental displacements where the applied torque T acts as an eigenvalue. It is observed that the first two stability equations are written only in terms of the in-plane displacements and the last three ones are expressed only in terms of the out-of-plane displacement components. Such decoupling is expected since the stretching-bending coupling stiffnesses are absent for an isotropic homogeneous material. Consequently, the last three equations are adequate to analyse the buckling load and shape of the annular plate subjected to torque.

5. Solution procedure

Since the geometry of the plate is periodic (a complete annular plate which occupies the domain $0 < \theta < 2\pi$), the displacement components and cross sections rotations should be periodic functions [16, 17, 20, 21, 24]. Therefore each of these

components take the form

$$\begin{aligned}
 w_0^1(r, \theta) &= W_n^c(r) \cos(n\theta) + W_n^s(r) \sin(n\theta), \\
 \varphi_r^1(r, \theta) &= \Phi_n^c(r) \cos(n\theta) + \Phi_n^s(r) \sin(n\theta), \\
 \varphi_\theta^1(r, \theta) &= \Psi_n^c(r) \cos(n\theta) + \Psi_n^s(r) \sin(n\theta),
 \end{aligned} \tag{20}$$

where number of nodal diameters is denoted by n . Inserting the Eqs. (20) into the last three governing equations (19) and collecting the coefficients $\sin(n\theta)$ and $\cos(n\theta)$, separately, the following six homogeneous coupled ordinary differential equations are obtained

$$\begin{aligned}
 &A_{66} \left(\Phi_{n,r}^c + \frac{n}{r} \Psi_n^s + \frac{1}{r} \Phi_n^c - \frac{n^2}{r^2} W_n^c + W_{n,rr}^c + \frac{1}{r} W_{n,r}^c \right) \\
 &\quad + \frac{nT}{\pi r^3} \left(W_{n,r}^s - \frac{1}{r} W_{n,r}^s \right) = 0, \\
 &A_{66} \left(\Phi_{n,r}^s + \frac{n}{r} \Psi_n^c + \frac{1}{r} \Phi_n^s - \frac{n^2}{r^2} W_n^s + W_{n,rr}^s + \frac{1}{r} W_{n,r}^s \right) \\
 &\quad - \frac{nT}{\pi r^3} \left(W_{n,r}^c - \frac{1}{r} W_{n,r}^c \right) = 0, \\
 &D_{11} \left(\Phi_{n,rr}^c + \frac{1}{r} \Phi_{n,r}^c + \frac{n}{r} \Psi_{n,r}^s - \frac{1}{r^2} \Phi_n^c - \frac{n}{r^2} \Psi_n^s \right) \\
 &\quad + D_{66} \left(-\frac{n^2}{r^2} \Phi_n^c - \frac{n}{r} \Psi_{n,r}^s - \frac{n}{r^2} \Psi_n^s \right) - A_{66} \left(\Phi_n^c + W_{n,r}^c \right) = 0, \\
 &D_{11} \left(\Phi_{n,rr}^s + \frac{1}{r} \Phi_{n,r}^s - \frac{n}{r} \Psi_{n,r}^c - \frac{1}{r^2} \Phi_n^s + \frac{n}{r^2} \Psi_n^c \right) \\
 &\quad + D_{66} \left(-\frac{n^2}{r^2} \Phi_n^s + \frac{n}{r} \Psi_{n,r}^c + \frac{n}{r^2} \Psi_n^c \right) - A_{66} \left(\Phi_n^s + W_{n,r}^s \right) = 0, \\
 &D_{11} \left(-\frac{n}{r} \Phi_{n,r}^c - \frac{n}{r^2} \Phi_n^c - \frac{n^2}{r^2} \Psi_n^s \right) + D_{66} \left(-\frac{n}{r^2} \Phi_n^c + \frac{n}{r} \Phi_{n,r}^c + \frac{1}{r} \Psi_{n,r}^s \right. \\
 &\quad \left. - \frac{1}{r^2} \Psi_n^s + \Psi_{n,rr}^s \right) - A_{66} \left(\Psi_n^s - \frac{n}{r} W_n^c \right) = 0, \\
 &D_{11} \left(\frac{n}{r} \Phi_{n,r}^s + \frac{n}{r^2} \Phi_n^s - \frac{n^2}{r^2} \Psi_n^c \right) + D_{66} \left(\frac{n}{r^2} \Phi_n^s - \frac{n}{r} \Phi_{n,r}^s + \frac{1}{r} \Psi_{n,r}^c \right. \\
 &\quad \left. - \frac{1}{r^2} \Psi_n^c + \Psi_{n,rr}^c \right) - A_{66} \left(\Psi_n^c + \frac{n}{r} W_n^s \right) = 0.
 \end{aligned} \tag{21}$$

The following dimensionless quantities are introduced and are used in the rest of the work

$$\begin{aligned} \mu &= \frac{2}{1-\nu}, & s &= \frac{r}{a}, & \delta &= \frac{h}{a}, & \beta &= \frac{b}{a}, \\ \bar{W}^s &= \frac{W^s}{a}, & \bar{W}^c &= \frac{W^c}{a}, & \tau &= \frac{12(1-\nu^2)T}{Eh^3}. \end{aligned} \quad (22)$$

With the aid of the newly defined parameters (22), stability equations (21) change to

$$\begin{aligned} \Phi_{n,s}^c + \frac{1}{s}\Phi_n^c + \frac{n}{s}\Psi_n^s + \bar{W}_{n,ss}^c + \frac{1}{s}\bar{W}_{n,s}^c - \frac{n^2}{s^2}\bar{W}_n^c \\ + \frac{1}{12\pi s^3}n\mu\delta^2\tau\left(\bar{W}_{n,s}^s - \frac{1}{s}\bar{W}_{n,s}^s\right) &= 0, \\ \Phi_{n,s}^s + \frac{1}{s}\Phi_n^s - \frac{n}{s}\Psi_n^c + \bar{W}_{n,ss}^s + \frac{1}{s}\bar{W}_{n,s}^s - \frac{n^2}{s^2}\bar{W}_n^s \\ - \frac{1}{12\pi s^3}n\mu\delta^2\tau\left(\bar{W}_{n,s}^c - \frac{1}{s}\bar{W}_{n,s}^c\right) &= 0, \\ \frac{\delta^2}{12}\left(\mu\Phi_{n,ss}^c + \frac{\mu}{s}\Phi_{n,s}^c - \left(\frac{12}{\delta^2} + \frac{\mu+n^2}{s^2}\right)\Phi_n^c + \frac{n}{s}(\mu-1)\Psi_n^s\right. \\ \left. - \frac{n}{s^2}(\mu+1)\Psi_n^s\right) - \bar{W}_{n,s}^c &= 0, \\ \frac{\delta^2}{12}\left(\mu\Phi_{n,ss}^s + \frac{\mu}{s}\Phi_{n,s}^s - \left(\frac{12}{\delta^2} + \frac{\mu+n^2}{s^2}\right)\Phi_n^s - \frac{n}{s}(\mu-1)\Psi_n^c\right. \\ \left. + \frac{n}{s^2}(\mu+1)\Psi_n^c\right) - \bar{W}_{n,s}^s &= 0, \\ \frac{\delta^2}{12}\left(-\frac{n}{s}(\mu-1)\Phi_{n,s}^c - \frac{n}{s^2}(\mu+1)\Phi_n^c + \Psi_{n,ss}^s + \frac{1}{s}\Psi_n^s\right. \\ \left. - \left(\frac{12}{\delta^2} + \frac{\mu n^2 + 1}{s^2}\right)\Psi_n^s\right) + \frac{n}{s}\bar{W}_n^c &= 0, \\ \frac{\delta^2}{12}\left(\frac{n}{s}(\mu-1)\Phi_{n,s}^s + \frac{n}{s^2}(\mu+1)\Phi_n^s + \Psi_{n,ss}^c + \frac{1}{s}\Psi_n^c\right. \\ \left. - \left(\frac{12}{\delta^2} + \frac{\mu n^2 + 1}{s^2}\right)\Psi_n^c\right) - \frac{n}{s}\bar{W}_n^s &= 0. \end{aligned} \quad (23)$$

Six highly coupled are provided in the above equations. These equations are homogeneous and have non-constant coefficients. Obtaining the exact solution for these equations, even if exists, is not straightforward. Therefore, a numerical strategy is preferred in this study. Generalised differential quadrature (GDQ) method as a pow-

erful tool is used to discretise the partial differential equations (23). The process is not repeated in here, meanwhile one may refer to the available works, see e.g. [25].

Distribution of nodal points is one of the main parameters in the GDQ method. Distribution according to Chebyshev-Gauss-Lobatto rule has shown excellent accuracy. In the current research also Chebyshev-Gauss-Lobatto distribution grid is used which yields

$$s_i = \beta + \frac{1 - \beta}{2} \left\{ 1 - \cos \left(\frac{i - 1}{N - 1} \pi \right) \right\}, \quad i = 1, 2, \dots, N \quad (24)$$

here the number of nodal points in GDQ method is denoted by N . Upon applying the GDQ method to Eqs. (23), a linear system of equations is achieved where the eigenvalue parameter is τ . After imposing the boundary conditions the eigenvalue problem takes the form

$$(\mathbf{K}_E - \tau \mathbf{K}_G) \mathbf{X} = 0. \quad (25)$$

In Eq. (25), the elastic stiffness matrix is denoted by \mathbf{K}_E while the geometric stiffness matrix induced by uniform torque $\tau = 1$ is denoted by \mathbf{K}_G . The mentioned system should be solved as eigenvalue problem to reach the critical buckling torque, critical buckling circumferential lode number and also buckling shape of the annular plate.

6. Numerical results and discussion

The process provided in the previous sections is used herein to discuss the critical states of an annular plate under the action of torque. In this section, the nondimensional torque parameter is introduced according to the definition of Irie et al. [6] which is equal to

$$\lambda_{cr} = \frac{1}{2\pi} \tau_{cr} = \frac{6(1 - \nu^2)T}{\pi E h^3}. \quad (26)$$

All of the numerical results and inputs data are in a dimensionless form and therefore the elasticity modulus of the plate is not needed to be known, however, Poisson's ratio affects the numerical results and is chosen as $\nu = 0.3$.

The following convention is established for the boundary conditions. For instance, an F-S plate indicates an annular plate which is free at inner edge while is simply-supported at the outer edge. After examination of convergence of the critical buckling load parameter up to three digits, the number of nodal points in the generalised differential quadrature method is set equal to $N = 32$ point.

For the case of thin annular plates, a comparison study is provided firstly. Afterwards, the critical buckling torques and the associated mode numbers are obtained for shear deformable annular plates with various combinations of boundary conditions.

6.1. Comparison studies

Comparison study of this research is confined to the case of thin annular plates. Irie et al. [6] reported the critical buckling torque and its associated mode number for thin plates with 8 different combinations of boundary conditions. This comparison is performed in Table 1. To model a thin plate the thickness to radius ratio is set as $\delta = 0.001$. As seen, both critical buckling torques and the number of nodal diameters at the onset of buckling are in reasonable agreement with the results of Irie et al. [6] which are obtained via a Ritz method.

Table 1.

Comparison of the non-dimensional critical buckling torque parameter λ_{cr} with those of Irie et al. [6]. Number of nodal diameters at the onset of buckling is provided in parenthesis

B.Cs.	Source	$\beta = 0.1$	$\beta = 0.2$	$\beta = 0.3$	$\beta = 0.4$	$\beta = 0.5$	$\beta = 0.6$	$\beta = 0.7$
C-C	Present	17.454(2)	35.982(3)	61.955(3)	106.271(4)	186.051(6)	341.101(7)	697.480(11)
	Irie et al. [6]	17.55(2)	36.02(3)	61.97(3)	106.3(4)	186.1(6)	341.2(7)	697.7(11)
S-S	Present	11.288(1)	21.323(2)	37.083(2)	63.401(3)	110.620(4)	202.305(5)	414.444(7)
	Irie et al. [6]	11.38(1)	21.35(2)	37.10(2)	63.41(3)	110.6(4)	202.3(5)	414.5(7)
C-S	Present	15.346(2)	29.353(2)	51.052(3)	87.262(4)	150.108(5)	273.920(6)	556.735(9)
	Irie et al. [6]	15.41(2)	29.37(2)	51.06(3)	87.27(4)	150.1(5)	274.0(6)	556.8(9)
S-C	Present	13.899(2)	25.800(2)	47.149(3)	81.310(3)	142.799(4)	262.297(6)	541.256(9)
	Irie et al. [6]	14.05(2)	25.85(2)	47.18(3)	81.33(3)	142.8(4)	262.3(6)	541.4(9)
F-C	Present	3.326(1)	6.026(1)	10.536(1)	19.304(1)	31.939(2)	59.440(3)	121.828(4)
	Irie et al. [6]	3.436(1)	6.092(1)	10.60(1)	19.37(1)	32.05(2)	59.63(3)	122.1(4)
F-S	Present	2.784(1)	4.6384(1)	7.282(1)	11.528(1)	18.991(1)	33.604(1)	63.959(2)
	Irie et al. [6]	2.905(1)	4.701(1)	7.330(1)	11.57(1)	19.03(1)	33.64(1)	64.03(2)
C-F	Present	5.134(1)	8.307(2)	12.782(2)	21.286(2)	35.763(3)	64.832(4)	128.774(5)
	Irie et al. [6]	5.137(1)	8.324(2)	12.80(2)	21.30(2)	35.80(3)	64.91(4)	128.9(5)
S-F	Present	2.875(1)	4.686(1)	7.319(1)	11.485(2)	17.252(2)	28.791(2)	55.761(2)
	Irie et al. [6]	2.811(1)	4.689(1)	7.319(1)	11.50(2)	17.26(2)	28.79(2)	55.73(2)

6.2. Parametric studies

After validating the present formulation for the case of thin plates, results are given for the case of moderately thick and thick plates.

Table 2 provides the critical buckling torque parameter for different combinations of boundary conditions, different thickness to radius ratios, and various inner to outer radius ratios. Numerical results from this study reveal that, for all types of boundary conditions, as the inner radius increases (β parameter increases) the critical buckling torque increases. Such trend is expected since the local flexural rigidity of the boundary conditions is more sensed when two boundaries are close to each other. Also, for different combinations of boundary conditions with the increase in the inner radius, number of nodal diameters also increases. It is observed that the

Table 2.

Non-dimensionless critical torque parameter λ_{cr} in annular shaped plates with different combinations of boundary conditions, various inner to outer radius ratios, and thickness to outer radius ratios. The number of nodal diameters is denoted in parenthesis

B.Cs.	δ	$\beta = 0.1$	$\beta = 0.2$	$\beta = 0.3$	$\beta = 0.4$	$\beta = 0.5$	$\beta = 0.6$	$\beta = 0.7$
C-C	0.001	17.454(2)	35.982(3)	61.955(3)	106.271(4)	186.051(6)	341.101(7)	697.480(11)
	0.02	16.808(2)	35.041(3)	60.431(3)	103.241(4)	178.986(6)	322.848(8)	635.728(11)
	0.05	14.229(2)	30.993(3)	53.758(3)	90.260(4)	150.414(6)	254.246(8)	444.826(11)
	0.10	9.144(2)	22.134(3)	39.261(3)	63.654(4)	98.436(6)	149.938(8)	223.078(13)
C-S	0.001	15.346(2)	29.353(2)	51.052(3)	87.262(4)	150.108(5)	273.920(6)	556.735(9)
	0.02	14.872(2)	28.775(2)	50.065(3)	85.337(4)	145.946(5)	263.448(6)	521.530(9)
	0.05	12.925(2)	26.181(2)	45.615(3)	76.769(4)	128.017(5)	220.267(7)	396.431(10)
	0.10	8.752(2)	20.111(2)	35.135(3)	57.421(4)	90.769(5)	141.452(7)	217.010(11)
S-C	0.001	13.899(2)	25.800(2)	47.149(3)	81.310(3)	142.799(4)	262.297(6)	541.256(9)
	0.02	13.588(2)	25.439(2)	46.438(3)	79.979(3)	139.577(5)	253.409(6)	509.559(9)
	0.05	12.122(2)	23.696(2)	43.030(3)	73.685(3)	124.172(5)	215.782(6)	392.895(9)
	0.10	8.454(2)	19.012(2)	34.090(3)	56.361(4)	89.694(5)	140.687(7)	216.458(11)
S-S	0.001	11.288(1)	21.323(2)	37.083(2)	63.401(3)	110.620(4)	202.305(5)	414.444(7)
	0.02	11.117(1)	21.092(2)	36.729(2)	62.658(3)	108.910(4)	197.893(5)	399.325(7)
	0.05	10.298(1)	19.952(2)	34.976(2)	59.025(3)	100.749(4)	177.662(5)	334.526(8)
	0.10	8.084(2)	16.689(2)	29.912(2)	48.947(3)	79.632(4)	128.870(6)	207.371(10)
F-S	0.001	2.784(1)	4.6384(1)	7.282(1)	11.528(1)	18.991(1)	33.604(1)	63.959(2)
	0.02	2.658(1)	4.543(1)	7.176(1)	11.375(1)	18.743(1)	33.136(1)	62.637(2)
	0.05	2.382(1)	4.294(1)	6.907(1)	11.010(1)	18.160(1)	31.993(1)	59.267(2)
	0.10	1.889(1)	3.798(1)	6.335(1)	10.204(1)	16.815(1)	29.072(1)	51.450(2)
F-C	0.001	3.326(1)	6.026(1)	10.536(1)	19.304(1)	31.939(2)	59.440(3)	121.828(4)
	0.02	3.166(1)	5.895(1)	10.361(1)	18.937(2)	31.320(2)	57.961(3)	117.738(4)
	0.05	2.810(1)	5.551(1)	9.904(1)	17.899(2)	29.607(2)	53.709(3)	105.451(4)
	0.10	2.176(1)	4.820(1)	8.877(1)	15.565(2)	25.626(2)	44.210(3)	80.175(5)
S-F	0.001	2.875(1)	4.686(1)	7.319(1)	11.485(2)	17.252(2)	28.791(2)	55.761(2)
	0.02	2.857(1)	4.669(1)	7.293(1)	11.408(2)	17.121(2)	28.521(2)	55.029(2)
	0.05	2.772(1)	4.598(1)	7.203(1)	11.210(2)	16.776(2)	27.775(2)	52.875(2)
	0.10	2.522(1)	4.373(1)	6.914(1)	10.645(2)	15.806(2)	25.731(2)	47.254(2)
C-F	0.001	5.134(1)	8.307(2)	12.782(2)	21.286(2)	35.763(3)	64.832(4)	128.774(5)
	0.02	5.072(1)	8.223(2)	12.656(2)	21.068(2)	35.249(3)	63.523(4)	124.896(5)
	0.05	4.794(1)	7.932(2)	12.215(2)	20.276(2)	33.524(3)	59.195(4)	112.078(5)
	0.10	4.078(1)	7.181(2)	11.030(2)	18.125(2)	29.174(3)	49.133(4)	85.778(5)

critical buckling load parameter is highly dependent on the thickness ratio. Such effect is ignored in classical plate theory. The effect of thickness is more observed in plates with clamped edge and is less sensed in plates with free edge. Unlike the classical plate theory results, in the analysis under first-order shear deformation plate theory the number of nodal diameters is dependent on the thickness ratio. The fact

that thickness may change the buckled shape of the plate is observed for thick plates with small β ratio while for moderately thick plates with higher β ratios this condition is more severe. Consequently, to achieve a reliable design and distinguish the number of critical points in a plate, the Mindlin plate theory is preferred.

Figures 1 to 3 depict the buckled shape of, in order, C-C, F-C, and C-F plates with various β ratios where the δ ratio is set equal to 0.05. It is verified that buckled

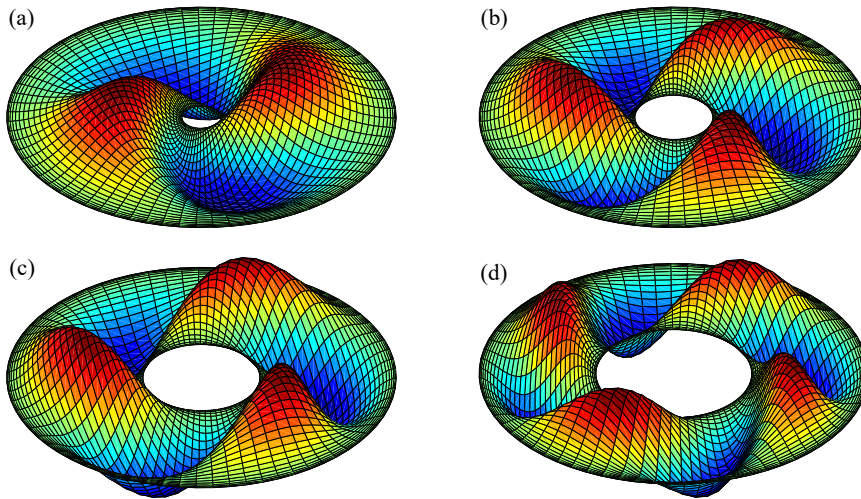


Fig. 1. Buckling configurations of C-C plates with $\delta = 0.05$ subjected to torque for various β ratios. (a) $\beta = 0.1, n = 2, \lambda_{cr} = 14.229$, (b) $\beta = 0.2, n = 3, \lambda_{cr} = 30.993$, (c) $\beta = 0.3, n = 3, \lambda_{cr} = 53.758$, (d) $\beta = 0.4, n = 4, \lambda_{cr} = 90.260$

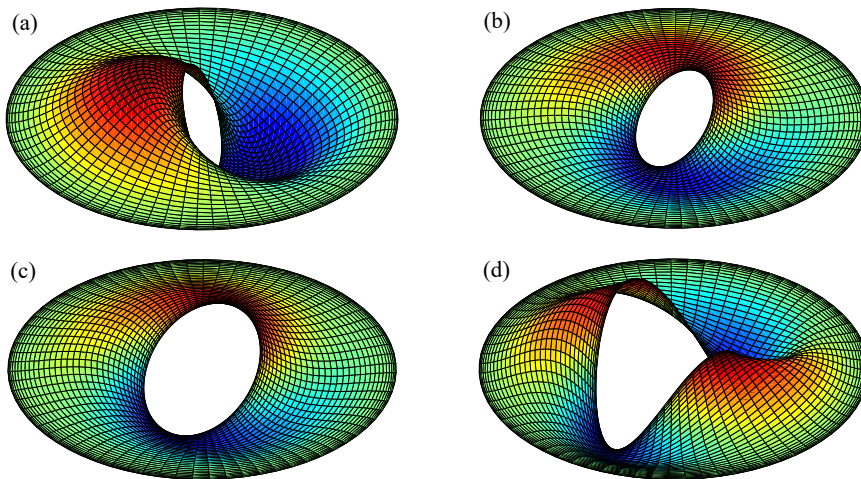


Fig. 2. Buckling configurations of F-C plates with $\delta = 0.05$ subjected to torque for various β ratios. (a) $\beta = 0.1, n = 1, \lambda_{cr} = 2.810$, (b) $\beta = 0.2, n = 1, \lambda_{cr} = 5.551$, (c) $\beta = 0.3, n = 1, \lambda_{cr} = 9.904$, (d) $\beta = 0.4, n = 2, \lambda_{cr} = 17.899$

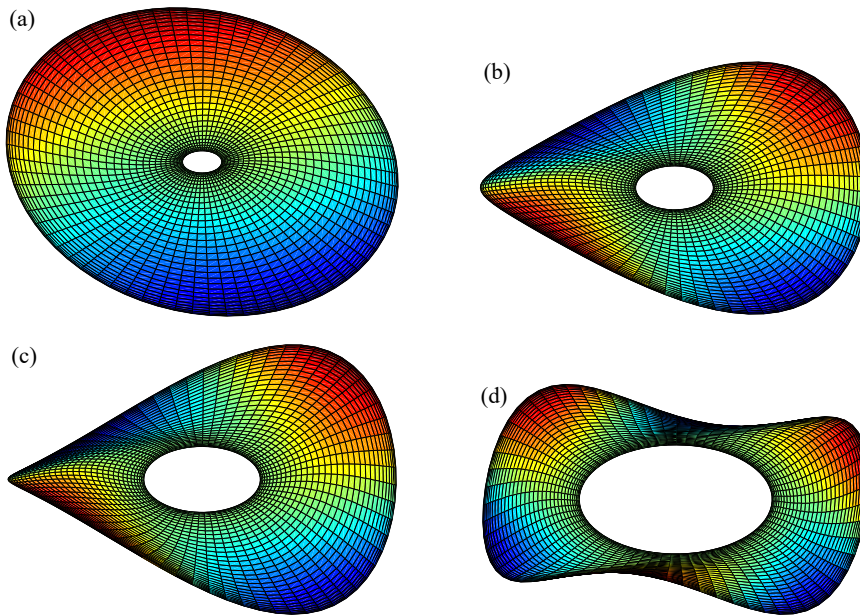


Fig. 3. Buckling configurations of C-F plates with $\delta = 0.05$ subjected to torque for various β ratios.

(a) $\beta = 0.1, n = 1, \lambda_{cr} = 4.794$, (b) $\beta = 0.2, n = 2, \lambda_{cr} = 7.932$, (c) $\beta = 0.3, n = 2, \lambda_{cr} = 12.215$,
 (d) $\beta = 0.5, n = 3, \lambda_{cr} = 33.524$

shape is highly dependent on the β ratio. Also it is seen that boundary conditions are satisfied at the supports of the plate.

7. Conclusion

An investigation is performed to analyse the asymmetrical buckling behaviour of annular plates subjected to a torque on the outer edge. Analysis is carried out using the first order shear deformation plate theory and the von-Kármán type of geometrical nonlinearity. The three partial differential equations are expressed in a new presentation which consists of six ordinary differential equations. These equations are solved as an eigenvalue problem using the generalised differential quadrature method. Followings are the general conclusions of the present study

- Buckling torque of the plate is highly dependent on the radii of the plate. In general, as the inner to outer radius ratio increases, the critical buckling torque increases too.

- The shape of the plate at the onset of buckling is highly dependent on the inner to outer radius ratio. For various combinations of boundary conditions, increasing the β ratio may increase the number of nodal diameters.

- Among the eight different combinations of boundary conditions, the buckling load from maximum to minimum belongs to C-C, C-S, S-C, S-S, C-F, F-C, S-F, and F-S plates.

- The critical buckling load depends on the thickness ratio. This fact is ignored in the classical plate theory. Dependency of the buckling load to thickness is more observed in plates with at least one edge clamped and is less revealed in plates with free edge.

- The number of nodal diameters which is a main factor in the buckled shape of the plate is highly dependent to the thickness ratio. This fact is ignored in analysis under classical plate theory. In general, increasing the thickness may increase the number of nodal diameters at the onset of buckling.

Manuscript received by Editorial Board, January 14, 2019;
final version, April 14, 2019.

References

- [1] W.R. Dean. The elastic stability of an annular plate. *Proceedings of the Royal Society of London. Series A, Containing Papers of a Mathematical and Physical Character*, 106(737):268–284, 1924. doi: [10.1098/rspa.1924.0068](https://doi.org/10.1098/rspa.1924.0068).
- [2] J. Tani and T. Nakamura. Dynamic stability of annular plates under pulsating torsion. *Journal of Applied Mechanics*, 47(3):595–600, 1980. doi: [10.1115/1.3153739](https://doi.org/10.1115/1.3153739).
- [3] J. Tani. Dynamic stability of orthotropic annular plates under pulsating torsion. *The Journal of the Acoustical Society of America*, 69(6):1688–1694, 1981. doi: [10.1121/1.385948](https://doi.org/10.1121/1.385948).
- [4] D. Durban and Y. Stavsky. Elastic buckling of polar-orthotropic annular plates in shear. *International Journal of Solids and Structures*, 18(1):51–58, 1982. doi: [10.1016/0020-7683\(82\)90015-4](https://doi.org/10.1016/0020-7683(82)90015-4).
- [5] T. Irie, G. Yamada, and M. Tsujino. Vibration and stability of a variable thickness annular plate subjected to a torque. *Journal of Sound and Vibration*, 85(2):277–285, 1982. doi: [10.1016/0022-460X\(82\)90522-3](https://doi.org/10.1016/0022-460X(82)90522-3).
- [6] T. Irie, G. Yamada, and M. Tsujino. Buckling loads of annular plates subjected to a torque. *Journal of Sound and Vibration*, 86(1):145–146, 1983. doi: [10.1016/0022-460X\(83\)90951-3](https://doi.org/10.1016/0022-460X(83)90951-3).
- [7] J. Zajęczkowski. Stability of transverse vibration of a circular plate subjected to a periodically varying torque. *Journal of Sound and Vibration*, 89(2):273–286, 1983. doi: [10.1016/0022-460X\(83\)90394-2](https://doi.org/10.1016/0022-460X(83)90394-2).
- [8] H. Doki and J. Tani. Buckling of polar orthotropic annular plates under internal radial load and torsion. *International Journal of Mechanical Sciences*, 27:429–437, 1985. doi: [10.1016/0020-7403\(85\)90033-5](https://doi.org/10.1016/0020-7403(85)90033-5).
- [9] M. Hamada and T. Harima. In-plane torsional buckling of an annular plate. *Bulletin of JSME*, 29(250):1089–1095, 1986. doi: [10.1299/jсме1958.29.1089](https://doi.org/10.1299/jсме1958.29.1089).
- [10] E. Ore and D. Durban. Elastoplastic buckling of annular plates in pure shear. *Journal of Applied Mechanics*, 56(3):644–651, 1989. doi: [10.1115/1.3176141](https://doi.org/10.1115/1.3176141).
- [11] Chang-Jun Cheng and Xiao-an Lui. Buckling and post-buckling of annular plates in shearing, Part I: Buckling. *Computer Methods in Applied Mechanics and Engineering*, 92(2):157–172, 1991. doi: [10.1016/0045-7825\(91\)90237-Z](https://doi.org/10.1016/0045-7825(91)90237-Z).
- [12] Chang-Jun Cheng and Xiao-an Lui. Buckling and post-buckling of annular plates in shearing, Part II: Post-buckling. *Computer Methods in Applied Mechanics and Engineering*, 92(2):173–191, 1991. doi: [10.1016/0045-7825\(91\)90238-2](https://doi.org/10.1016/0045-7825(91)90238-2).
- [13] P. Singhatanadgid and V. Ungbhakorn. Scaling laws for buckling of polar orthotropic annular plates subjected to compressive and torsional loading. *Thin-Walled Structures*, 43(7):1115–1129, 2005. doi: [10.1016/j.tws.2004.11.004](https://doi.org/10.1016/j.tws.2004.11.004).

- [14] T.X. Wu. Analytical study on torsional vibration of circular and annular plate. *Journal of Mechanical Engineering Science*, 220(4):393–401, 2006. doi: [10.1243/09544062JMES167](https://doi.org/10.1243/09544062JMES167).
- [15] R. Margetic, V. Glavardanov, and D. Radomirovic. Asymmetric vibrations and stability of a rotating annular plate loaded by a torque. *Meccanica*, 42(6):537–546, 2007. doi: [10.1007/s11012-007-9080-8](https://doi.org/10.1007/s11012-007-9080-8).
- [16] S.E. Ghiasian, Y. Kiani, M. Sadighi, and M.R. Eslami. Thermal buckling of shear deformable temperature dependent circular annular FGM plates. *International Journal of Mechanical Sciences*, 81:137–148, 2014. doi: [10.1016/j.ijmecsci.2014.02.007](https://doi.org/10.1016/j.ijmecsci.2014.02.007).
- [17] H. Bagheri, Y. Kiani, and M.R. Eslami. Asymmetric thermal buckling of temperature dependent annular FGM plates on a partial elastic foundation. *Computers & Mathematics with Applications*, 75(5):1566–1581, 2018. doi: [10.1016/j.camwa.2017.11.021](https://doi.org/10.1016/j.camwa.2017.11.021).
- [18] H. Bagheri, Y. Kiani, and M.R. Eslami. Asymmetric compressive stability of rotating annular plates. *European Journal of Computational Mechanics*, 2019. doi: [10.1080/17797179.2018.1560989](https://doi.org/10.1080/17797179.2018.1560989).
- [19] J.N. Reddy. *Mechanics of Laminated Composite Plates and Shells, Theory and Application*. CRC Press, 2nd Edition, 2003.
- [20] H. Bagheri, Y. Kiani, and M.R. Eslami. Asymmetric thermal buckling of annular plates on a partial elastic foundation. *Journal of Thermal Stresses*, 40(8):1015–1029, 2017. doi: [10.1080/01495739.2016.1265474](https://doi.org/10.1080/01495739.2016.1265474).
- [21] H. Bagheri, Y. Kiani, and M.R. Eslami. Asymmetric thermo-inertial buckling of annular plates. *Acta Mechanica*, 228(4):1493–1509, 2017. doi: [10.1007/s00707-016-1772-5](https://doi.org/10.1007/s00707-016-1772-5)
- [22] D.O. Brush and B.O. Almroth. *Buckling of Bars, Plates, and Shells*, McGraw-Hill, New York, 1975.
- [23] M.R. Eslami. *Thermo-Mechanical Buckling of Composite Plates and Shells*, Amirkabir University Press, Tehran, 2010.
- [24] Y. Kiani Y and M.R. Eslami. An exact solution for thermal buckling of annular FGM plates on an elastic medium. *Composites Part B: Engineering*, 45(1):101–110, 2013. doi: [10.1016/j.compositesb.2012.09.034](https://doi.org/10.1016/j.compositesb.2012.09.034).
- [25] F. Tornabene, N. Fantuzzi F. Ubertini, and E. Viola. Strong formulation finite element method based on differential quadrature: a survey. *Applied Mechanics Reviews*, 67(2):020801–020801-55, 2015. doi: [10.1115/1.4028859](https://doi.org/10.1115/1.4028859).